


RESEARCH ARTICLE | SEPTEMBER 13 2023

Damage analysis in a composite by X-ray tomography methods using the structure tensor

Mikhail Bannikov; Yuriy Bayandin ; Oleg Naimark; Eduard Pruel; Konstantin Kuper



AIP Conf. Proc. 2899, 020010 (2023)

<https://doi.org/10.1063/5.0162973>



View
Online



Export
Citation

CrossMark



APL Energy
First Articles Online!
Read Now



Damage Analysis in a Composite by X-ray Tomography Methods Using the Structure Tensor

Mikhail Bannikov¹, Yuriy Bayandin^{1,a)}, Oleg Naimark¹, Eduard Pruel² and Konstantin Kuper³

¹*Institute of Continuous Media Mechanics, UB RAS, 1, Ac. Korolev str., Perm, Russia, 614013*

²*Lavrentyev Institute of Hydrodynamics, SB RAS, 15, Lavrentyev av., Novosibirsk, Russia, 630090*

³*Budker Institute of Nuclear Physics, SB RAS, 11, Lavrentyev av., Novosibirsk, Russia, 630090*

^{a)}Corresponding author: buv@icmm.ru

Abstract. The aim of the work is to analyze X-ray synchrotron microtomography data obtained for polymers reinforced with carbon fibers and to reveal the multiscale regularities of damage development caused by both the technological manufacturing process and the deformation contribution to the loading process of a sample of layered polymer composite material. It is known that the orientation distribution determined by the fiber stacking technology causes the mechanical properties of composites, and the production quality primarily determines the performance characteristics of material. Generally accepted methods for characterizing composites involve identifying fibers as individual objects, which requires high-resolution X-rays and large computational resources. This paper investigates damage analysis based on the field determination of the structure tensor of a representative volume of the composite, which makes it possible to determine both technological defects and accumulated damage during the deformation process.

INTRODUCTION

The structure tensor, which in its components has the sense of a second-moment matrix and represents the gradient of the studied distribution field, is currently gaining popularity for morphological data analysis (2D and 3D). It describes the distribution of the gradient in a given vicinity around a point and makes the structure spatial invariant with respect to the observation coordinates. The structure tensor is often used in image processing and computer vision. In particular, morphology analysis using the structure tensor is applied to micro-CT imaging data [1,2].

Previously, the authors of the work performed a study of the structure of a loaded specimen of carbon fiber-reinforced polymer and obtained integral characteristics of damages (pores) in the composite material on the basis of microtomography data [3]. Synchrotron radiation of charged particle gas pedal VEPP-3 (Institute of Nuclear Physics SB RAS, Novosibirsk, Russia) was used as a X-ray source [4]. A field analysis of the morphology of the composite structure before and after deformation provides more complete information about the distribution of discontinuities and defects. In the present study, an analysis based on the application of the structure tensor for micro-CT imaging data obtained from representative sample volumes cut from the initial state of the specimen and the loaded specimen was applied. Based on the obtained structure tensor field, the parameters characterizing the microstructure were calculated: averaged intensity, anisotropy coefficient, determinant of the tensor, trace of the tensor. The differences between the initial and deformed states of the composite were determined by characteristic differences in the distribution of these parameters.

COMPOSITE SPECIMEN LOADING EXPERIMENT

In order to determine the processes of damage accumulation near stress concentrators during deformation of a polymer composite specimen, quasi-static deformation studies of specimens with a hole, combined with the analysis of deformation fields by DIC data, were carried out. Composite material specimens in the form of a flat strip (Fig. 1) were made of carbon fabric CW200-TW2/2 twill woven with an epoxy matrix, with an even number of pairs of layers with the orientation of the base to the axis of loading at angles of 0/45/90/-45 degrees.

Quasi-static tension of the polymer composite specimens was performed at a constant loading rate of 1 mm per minute until rupture. A Shimadzu AG-Xplus testing machine was used for loading, which provides linear movement of an active gripper with a specified constant loading rate and load measurement with an error of no more than $\pm 1\%$ of the measured value. The same material was glued to the specimen to ensure good fixation in the grips of the loading machine. The specimen was installed in the grips of the testing machine so that its longitudinal axis coincided with the axis of load application. The force application conditions in the grips did not cause failure of the specimens in the area of attachment and excluded slippage in the grips. Stress concentrators in the form of holes in the central area of the specimen reduced the ultimate load to failure compared to a specimen without a concentrator by 30%.

To investigate damage distribution in the area of stress concentrators, the specimens were loaded to 85% of the failure stress value and the experiment was stopped. In the areas with the largest and smallest local strain (red and blue regions in Fig. 1, respectively) samples were drilled out of the specimens with a hollow diamond drill (diameter of 6 mm) for analysis by X-ray microtomography.

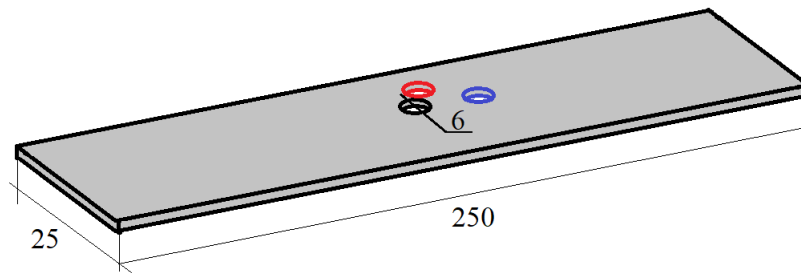


FIGURE 1. Geometry of the specimen with hole and sample drilling locations for micro-CT analysis (red – in the area of the largest local strain, blue – in the area of the smallest local strain)

Images of the non-loaded specimen and the loaded specimen with cut samples are shown in Fig. 2.

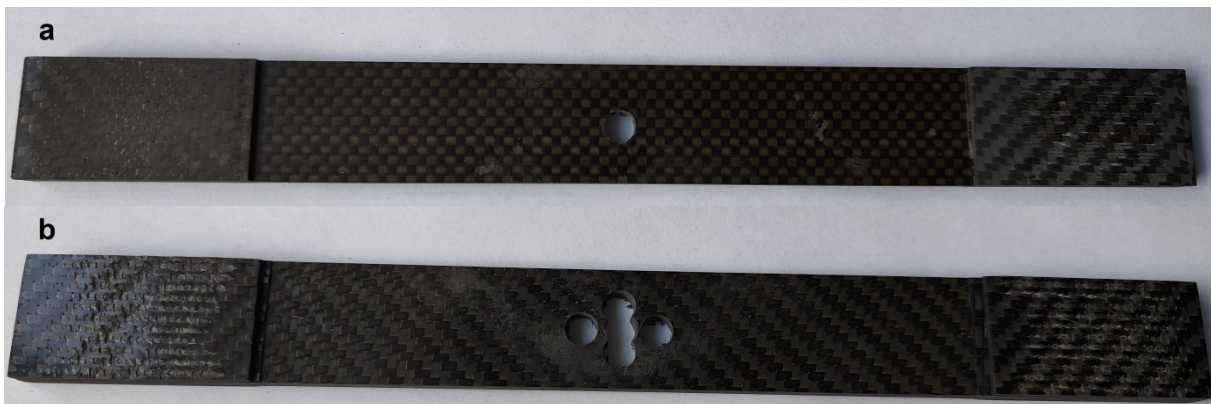


FIGURE 2. Specimens: (a) before loading; (b) after loading and cutting samples for micro-CT

STRUCTURE TENSOR ANALYSIS

Data analysis was implemented in the MathWorks MATLAB application package based on the structure tensor field definition. Figure 3 shows the characteristic initial images of the structure density isosurfaces for the deformed specimen. Figure 3b shows the presence of a large technological defect in the form of a pore between the layers of the composite.

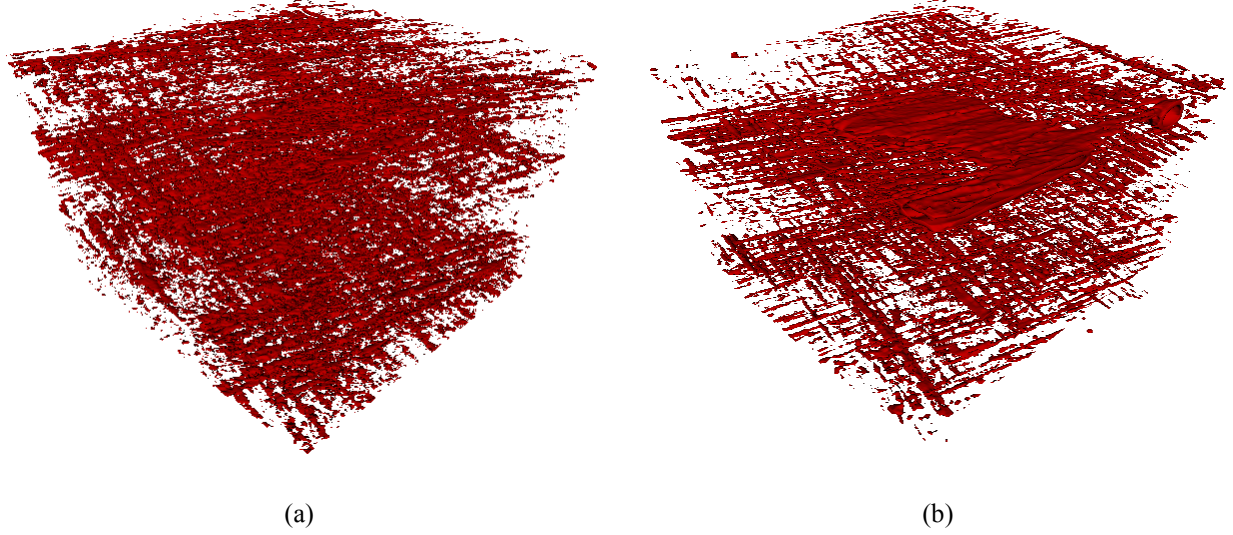


FIGURE 3. Isosurfaces of intensity: (a) region near the concentrator, (b) region with the defect

The structure tensor fields [1,2] for initial state samples and loaded samples were determined according to the following expressions

$$\alpha'_{ij}(x_1, x_2, x_3) = \begin{bmatrix} \left(\frac{\partial \rho}{\partial x_1} \right)^2 & \frac{\partial \rho}{\partial x_1} \frac{\partial \rho}{\partial x_2} & \frac{\partial \rho}{\partial x_1} \frac{\partial \rho}{\partial x_3} \\ \frac{\partial \rho}{\partial x_2} \frac{\partial \rho}{\partial x_1} & \left(\frac{\partial \rho}{\partial x_2} \right)^2 & \frac{\partial \rho}{\partial x_2} \frac{\partial \rho}{\partial x_3} \\ \frac{\partial \rho}{\partial x_3} \frac{\partial \rho}{\partial x_1} & \frac{\partial \rho}{\partial x_3} \frac{\partial \rho}{\partial x_2} & \left(\frac{\partial \rho}{\partial x_3} \right)^2 \end{bmatrix}, \quad (1)$$

where $\rho(x_1, x_2, x_3)$ is the intensity distribution, $\alpha'_{ij}(x_1, x_2, x_3)$ is the structure tensor field.

Then the averaging of the structure tensor field (1) in each point \bar{r} over a given window size $W(\bar{r})$ is performed

$$\alpha_{ij}(\bar{r}) = \langle \alpha'_{ij}(x_1, x_2, x_3) \rangle_{\bar{r}} = \iiint_{W(\bar{r})} \alpha'_{ij}(x_1, x_2, x_3) dx_1 dx_2 dx_3. \quad (2)$$

For the obtained structure tensor field in each point \bar{r} , the spectrum of the eigenvalues $\lambda_1, \lambda_2, \lambda_3$ of the component matrix (2) was determined, on the basis of which the parameters characterizing the microstructure were calculated: the anisotropy factor $\beta = 1 - \lambda_{\min} / \lambda_{\max}$, the tensor determinant $\det(\alpha_{ij}) = \lambda_1 \lambda_2 \lambda_3$ and the tensor trace $\text{sp}(\alpha_{ij}) = \lambda_1 + \lambda_2 + \lambda_3$.

RESULTS AND DISCUSSIONS

The probability density function [5] is widely used as a characteristic of complex systems. Using the above parameters, the probability density function (PDF) over the entire representative volume of each sample was studied. For example, the characteristic PDF versus different parameters for a representative sample volume near a stress concentrator are presented in Figs. 4 and 5.

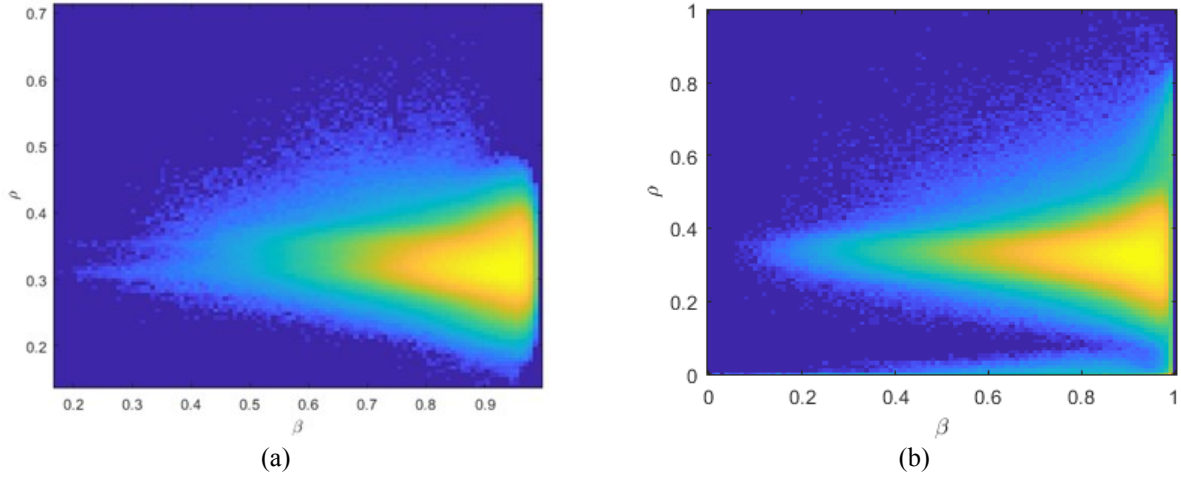


FIGURE 4. Probability density function versus anisotropy factor β and intensity ρ :
(a) initial sample; (b) sample with defect (large pore)

The probability density function in Fig. 5 is given as a function of the decimal logarithm of the determinant for a better illustration.

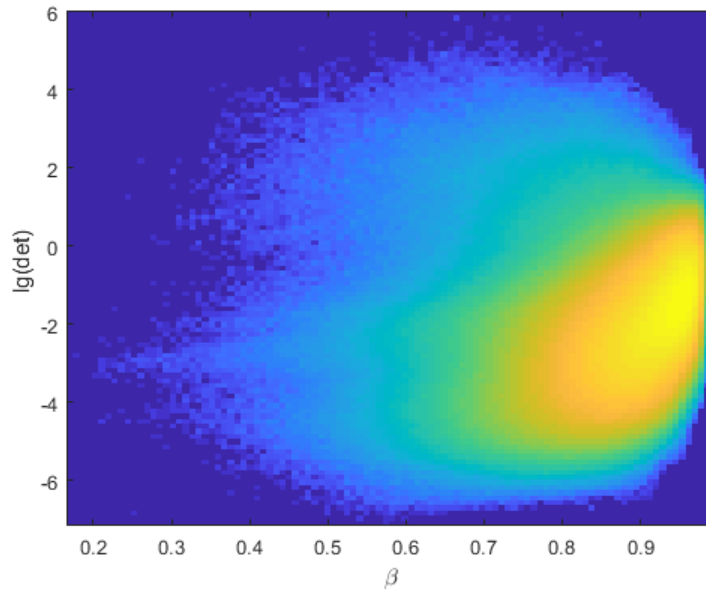


FIGURE 5. Probability density function versus anisotropy factor β and determinant

The dependences of the probability density functions are non-monotonic, and the differences between the original and loaded samples are evident at small scale levels. Therefore, another parameter was proposed for the study, defining the ratio of the structure tensor value as a gradient of the intensity field (e.g. trace tensor) to the average intensity value

$$\gamma = \frac{\Delta\rho}{\rho} = \frac{\text{sp}(\alpha_{ij})}{\rho}. \quad (3)$$

The equation (3) determines the dimensionless ratio of the intensity of the structure tensor (trace) and in geometric sense reflects the magnitude of intensity-to-intensity fluctuations. Figure 6 illustrates the difference in the dependence of the function on the new parameter for the original sample and the sample with the defect. The sample with initial state shows a power law of distribution with an index equal to -2 . This is due to the second-order derivative in formula (1) and in the form of a normalized sum of diagonal components of the structure tensor (2). For the sample with a defect the second power law is expressed on the PDF plot for $\lg(\gamma)$ greater than 7, which may be related to damage. Similar power laws for PDF have been observed in the fracture of brittle materials [6], including rocks materials [7].

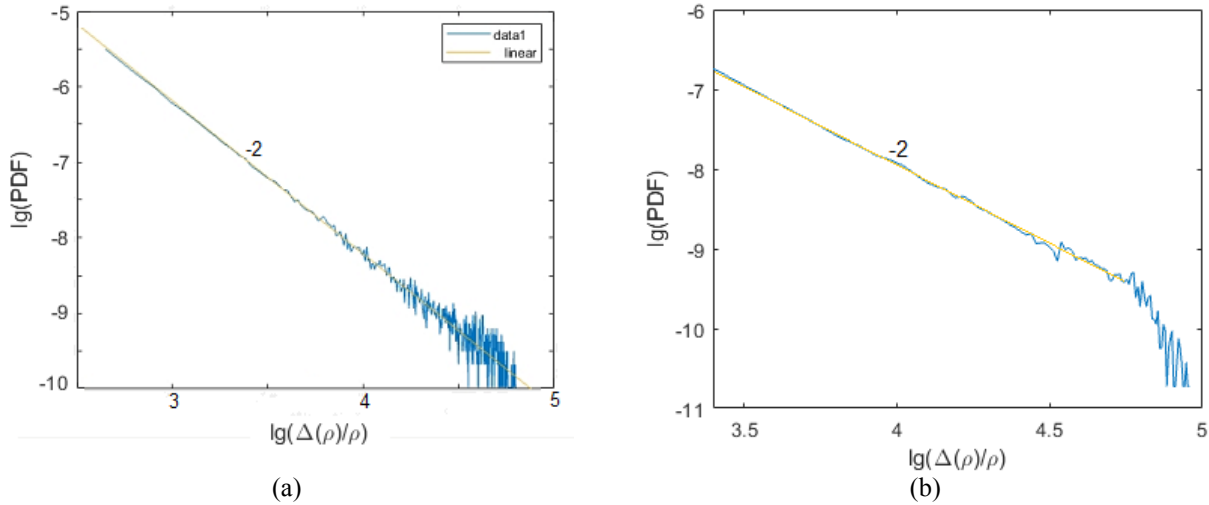


FIGURE 6. Probability density functions versus gamma parameter (3) in log-log coordinates: (a) initial sample; (b) sample with defect

CONCLUSION

Based on the results of the analysis of the probability density functions (PDF), it was found that the anisotropy factor as well as the sum of squares of the intensity derivatives (structure tensor trace) are sensitive parameters for damage detection. Additionally, it was found that in the case of detecting technological defects (initial discontinuities), the distribution functions become non-monotonic, which can also be reflected in the occurrence of deformation damage. The detection of a finer structure, including microdamage, requires an increase in the resolution of X-ray tomography.

ACKNOWLEDGMENTS

Experiments on quasi-static loading of specimens and subsequent microstructure analysis were carried out by M.B., Yu.B., and O.B. with financial support from the Russian Science Foundation (Project No. 21-79-30041). X-ray microtomography was performed by E.P. and K.K. on the equipment of the Budker Institute of Nuclear Physics of SB RAS and funded by the Ministry of Science and Higher Education of the Russian Federation (Project No. 075-15-2020-781).

REFERENCES

1. N. Nguyen, M. Mehdikhani, I. Straumit, L. Gorbatikh, L. Lessard, and S. Lomov, *Compos. A: Appl. Sci. Manuf.* **104**, 14–23 (2018).

2. R. Karamov, L. Martulli, M. Kerschbaum, I. Sergeichev, Y. Swolfs, and S. Lomov, [Comp. Str.](#) **235**, 111818 (2020).
3. A. M. Ignatova, A. N. Balakhnin, M. V. Bannikov, K. E. Kuper, A. S. Nikitiuk, and O. B. Naimark, [Procedia Struct. Integr.](#) **41**, 550–556 (2022).
4. A. N. Drobchik, V. V. Nikitin, M. I. Fokin, G. A. Dugarov, P. D. Shevchenko, A. L. Deriy, A. Yu. Manakov, K. E. Kuper, and A. A. Duchkov, [J. Synchrotron Radiat.](#) **29**(2), 515–521 (2022).
5. J. Chen, T. Liu, Z. Huang, and G. Su, [Int. J. Mod. Phys. B](#) **32**(03), 1850022 (2018).
6. I. A. Bannikova and S. V. Uvarov, [Procedia Struct. Integr.](#) **32**, 10–16 (2021).
7. I. A. Bannikova and S. V. Uvarov, [Procedia Struct. Integr.](#) **33**, 357–364 (2021).